



3D Assembly of All-Inorganic Colloidal Nanocrystals into Gels and Aerogels

Vladimir Sayevich, Bin Cai, Albrecht Benad, Danny Haubold, Luisa Sonntag, Nikolai Gaponik, Vladimir Lesnyak,* and Alexander Eychmüller

Abstract: We report an efficient approach to assemble a variety of electrostatically stabilized all-inorganic semiconductor nanocrystals (NCs) by their linking with appropriate ions into multibranched gel networks. These all-inorganic non-ordered 3D assemblies benefit from strong interparticle coupling, which facilitates charge transport between the NCs with diverse morphologies, compositions, sizes, and functional capping ligands. Moreover, the resulting dry gels (aerogels) are highly porous monolithic structures, which preserve the quantum confinement of their building blocks. The inorganic semiconductor aerogel made of 4.5 nm CdSe colloidal NCs capped with Γ^- ions and bridged with Cd^{2+} ions had a large surface area of $146 \text{ m}^2 \text{ g}^{-1}$.

Colloidal semiconductor nanocrystals (NCs) attract enormous scientific and technological interest owing to their size- and shape-tunable optical, electrical, and magnetic properties.^[1] Transferring these specific characteristics by their self-assembly into 3D superstructures will not only allow for bridging the macro- and nanodimensions, but also enable the creation of completely new properties as a result of their collective interparticle interactions.^[2] Gels and aerogels built from various colloidal NCs have recently been shown to provide such opportunities.^[3]

Nowadays, the assembly of a variety of nanoparticles, in particular, noble-metal and semiconductor NCs, into functional non-ordered architectures is rather well-developed and can easily be realized while maintaining the nanoscale properties. However, in many cases, the resulting gels still have to be further processed to improve properties that are relevant for the desired practical applications. For instance, the surface capping of NCs is a critical aspect in the fabrication of functional gels. Various organic molecules are generally employed as stabilizing ligands in the colloidal synthesis of such nanoparticles. These ligands lead to an increase in the amount of organic molecules in the gel structure and thus may hinder the accessibility of the active NC surface. The latter is of paramount importance for the application of these materials as catalysts. Further processing of the wet NC gels may cause the formation of multiple side

products from the organic ligands, leading to unpredictable changes in the properties of the final material.

Alternatively, inexpensive and very small inorganic ligands can efficiently replace the original organic molecules on the surface of the NCs, thus providing electrostatic stabilization in polar solvents. These new ligands have a high affinity to the surface of the NCs, preserving their electronic structure and photophysical characteristics.^[4] The diversity of available inorganic species enables the modulation of a wide variety of properties, including the type of conduction-dominating carrier and its mobility, the photoluminescence (PL), and the catalytic activity.^[5] Moreover, close-packed NC solids capped with appropriate inorganic ligands showed unprecedented electronic characteristics with strong coupling interactions, providing bright prospects for semiconductor technologies based on colloidal nanomaterials.^[4a,6]

These findings motivated us to develop a novel approach to form 3D non-ordered assemblies based on NCs capped with inorganic ligands. We explored an extensive series of all-inorganic semiconductor NCs with different morphologies, compositions, sizes, and capping ligands as building blocks for the formation of all-inorganic gels. In particular, we employed spherical NCs, nanorods, and nanoplatelets.

Our group previously developed a couple of strategies, such the mild and well-controllable destabilization of NC colloids^[7] and their linking by metal-ion-assisted complexation,^[8] to interconnect NCs with suitable ions, to obtain multibranched open networks. During the preparation of this paper, Milliron and co-workers reported the first successful fabrication of an all-inorganic gel based on CdSe NCs capped with complex $[\text{Ge}_2\text{Se}_6]^{4-}$ ligands through their coordination with Pt^{2+} ions.^[9] However, this gelation approach may affect the optoelectronic characteristics of the NC building blocks. Furthermore, unintentional cation exchange with the linking ions may also lead to undesirable modifications of the NC constituents in the gel.

Herein, we synthesized spherical colloidal CdSe, PbS, PbSe, and ZnO semiconductor NCs with narrow particle-size distributions as well as CdSe nanoplatelets and ZnO nanorods that were capped with native long-chain insulating organic ligands (for experimental details, see the Supporting Information). Subsequently, we completely replaced these molecules with different inorganic ligands, such as S^{2-} , I^- , Cl^- , F^- , and Ga/I and In/Cl complexes. Their nucleophilicity and high affinity towards the NC surfaces provide electrostatic stabilization for such colloidal dispersions in the polar solvent *N*-methylformamide (MFA) for a wide range of concentrations. Transmission electron microscopy (TEM) images of the

[*] V. Sayevich, B. Cai, A. Benad, D. Haubold, L. Sonntag, Prof. N. Gaponik, Dr. V. Lesnyak, Prof. A. Eychmüller
Physical Chemistry and Center for Advancing Electronics Dresden (cfaED), TU Dresden
Bergstrasse 66b, 01062 Dresden (Germany)
E-mail: vladimir.lesnyak@chemie.tu-dresden.de

Supporting information for this article can be found under:
<http://dx.doi.org/10.1002/anie.201600094>.

inorganic-ligand-stabilized NCs confirmed the retention of their sizes, shapes, and narrow size distributions after ligand exchange (Supporting Information, Figure S1). In solutions of the inorganic-ligand-capped NCs, the excitonic features of their optical absorption spectra were preserved (Figure S2). The disappearance of the infrared absorption bands related to the characteristic C–H stretching modes ($2700\text{--}3000\text{ cm}^{-1}$) of organic-ligand-capped NCs confirmed the complete removal of the original organic ligands (Figure S3), which is in agreement with our recent detailed studies of the inorganic functionalization of various NCs.^[4c,10] The successful functionalization of the NC surfaces with charged species was further confirmed by electrophoretic measurements, which revealed characteristic electrokinetic potentials (ξ) for these particles related to their surface charge density (Figure S4, Table S1).

In the next step, the NCs were assembled into 3D networks. To produce porous and multibranched gels, the choice of salts that contain appropriate coordinating cations was of high importance. Talapin and co-workers recently reported that Cd^{2+} ions showed the highest affinity among various studied cations towards the surface of S^{2-} -capped CdSe NCs, leading to the highest surface charge inversion.^[5] We assumed that the chemical similarity of these ions in this process is likely to play a crucial role. Therefore, the gelation of the inorganic-ligand-functionalized CdSe, PbSe, and ZnO NCs was induced by adding Cd^{2+} , Pb^{2+} , and Zn^{2+} ions, respectively, in the form of dehydrated acetate salts. Other salts with weakly nucleophilic anions, such as nitrates and perchlorates, can also be used, enabling the complete avoidance of organic residues in the resulting gels. Although these salts were successfully used to gelate $\text{CdSe}(\text{I}^-)$ NCs, their different solubilities in the chosen solvents or mixtures of solvents complicated comparative studies of the gelation of different NCs (see the Supporting Information). This gelation approach can also be extended by employing different cations for linking, as shown in our previous work.^[8b]

To induce the metal-ion-assisted assembly of $\text{CdSe}(\text{I}^-)$ NCs, we added a 0.2 M solution of cadmium acetate to

a 3 mg mL^{-1} NC dispersion in MFA, which corresponds to a final Cd^{2+} concentration of 20 mM. The gelation of other combinations of NCs and bridging ions was carried out in a similar way, but the efficiency of the conversion of the NCs into gels and the gelation time varied owing to some uncertainties in the determination of the NC concentrations, their different sizes, morphologies, or surface charge densities (Figure 1, Table S2).

Both concentrations, that of the linking cations and that of the NCs, played an important role in determining the kinetics of the network formation and the structure of the resulting gel. Reducing the concentration of either the linking cations or the NCs or both did not result in any signs of destabilization of the system within months. On the contrary, increasing the concentration of the Cd^{2+} ions or the $\text{CdSe}(\text{I}^-)$ NCs led to their immediate precipitation in the form of dense sediments. In turn, a balanced cation/NC ratio at appropriate concentrations yielded multibranched structures within one week with a gel conversion efficiency of approximately 80 % (i.e., 80 % of the initial NC content was transformed into the gel).

The advantage of using charged all-inorganic NCs as building blocks is their inclination to form gel networks through bridging by counterions independent of their size, composition, morphology, and even charge (Figure S5). For example, S^{2-} -capped CdSe NCs charge-inverted with Cd^{2+} (i.e., positively charged “ $\text{CdSe}(\text{S}^{2-})(\text{Cd}^{2+})$ ”) may be gelled by the addition of S^{2-} linkers. This can be explained as follows. The NCs may be considered as lyophobic colloids, which are thermodynamically metastable (with respect to the bulk solid) and rendered “stable” only in a kinetic sense. The kinetics of gelation (coagulation) will mainly be determined by overcoming the potential energy barrier controlling the NC stability, that is, their repulsion. After the addition of the linking agent, the charged cations adsorb on a few sites of the NC surface, which is negatively charged, increasing the attractive potential contribution. Furthermore, to guarantee effective bridging and the simultaneously occurring charge neutralization, there ought to be sufficient bare space on the surface of neighboring NCs to promote the effective adsorp-

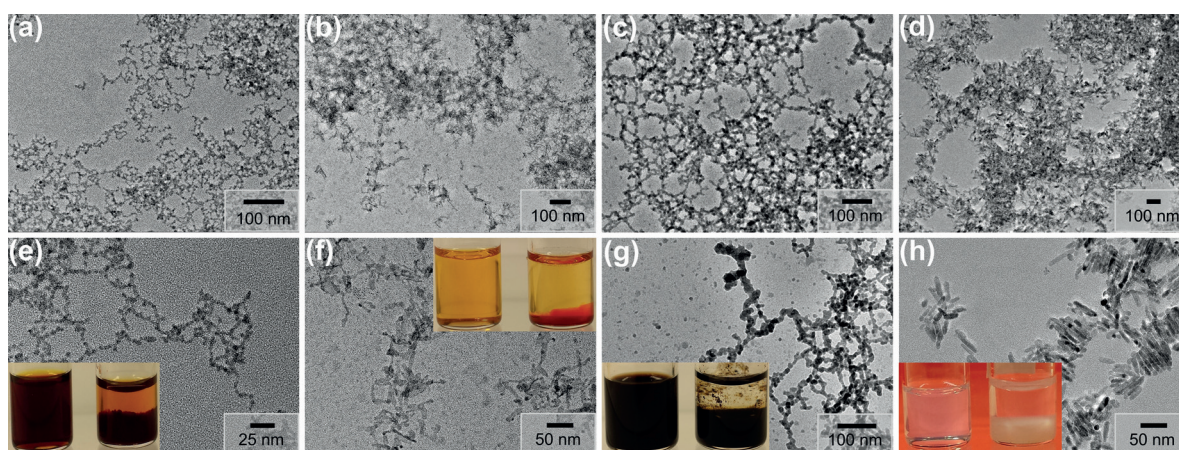


Figure 1. TEM images of a variety of all-inorganic NC gels formed using appropriate counterions: $\text{CdSe}(\text{I}^-)$ NCs/ Cd^{2+} (a, e); CdSe nanoplatelets- $(\text{I}^-)/\text{Cd}^{2+}$ (b, f); $\text{PbSe}(\text{I}^-)$ NCs/ Pb^{2+} (c, g); ZnO nanorods(F^-)/ Zn^{2+} (d, h). The insets are photographs of the corresponding NC dispersions before (left) and after (right) gelation.

tion of positively charged areas during particle approach, preferably with enough space for more than one contact.

When the NC concentration is low, the probability of particle–particle encounters is also low, and at a high enough counterion concentration, the reversion of the NC surface charge and the formation of a stable suspension may occur. On the other hand, at high ion and NC concentrations, coagulation is fast, yielding compact and dense aggregates by bridging through the larger average number of cations attached to each particle.^[5] Therefore, only optimal NC and counterion concentrations result in the formation of open porous structures. With the gelation time, the local coordination environment of the bridging ions can vary across the NC network, which is accompanied by its reconstruction and the strengthening of bonds between the structural units. This process is known as aging, and depends on the nature of the structural units and ligands, their concentrations, and surface charge densities, for example, and varies from sample to sample (Table S2).

The aging time is of high importance for these gel systems as they do not possess excellent complexation capabilities. We assume that during the aging process, the formation of strong covalent bonds, such as I–Cd–I and Se–Cd–Se, takes place, accompanied by interfusion of the NCs, which determines the rigid framework of the gel structure (Figure 2). The lack of reversibility observed upon using strong complexation agents (EDTA or its salts) additionally confirmed the formation of strong bonds between the NCs. Moreover, the gelation of the CdSe(I[−]) NCs could also be initiated by other ions such as Pb²⁺ and Zn²⁺, but the kinetics of gelation and optical properties of the resulting gels differed from those of the Cd-linked particles. As the colloidal stability of charged NCs strongly depends on the concentration of the electrolyte (known as the Schulze–Hardy rule), we performed a control experiment by adding a 60 mM solution of NaOAc with an ionic strength identical to 20 mM Cd(OAc)₂ to the CdSe(I[−]) NCs. In this case, we did not observe any aggregation of the NCs, which confirms that their bridging is induced by linking via Cd²⁺ ions and not just due to the increased ionic strength of the solution. Nevertheless, we also considered the possibility of gel formation by changes in the ionic strength, the

dielectric constant, and the temperature as ways to change the magnitude of the surface charge density and the extent of the electrical double layer and thus to induce gelation.

Furthermore, we monitored the aggregation of the CdSe(I[−]) NCs by TEM in the early stages of gelation. We first observed the formation of chains (after 24 h) with subsequent branching and the generation of more complex fractal aggregates (after 48 h), which acted as building blocks for the construction of a well-connected gel network (after 1 week; Figure 2, Figure S6). The NCs were randomly oriented in these gels, as revealed by high-resolution TEM imaging (Figure 2d, Figure S7). Further detailed studies will be needed to elucidate the gelation driving force; the different contributions of the various components to the total interaction potential could be analyzed by using the Derjaguin–Landau–Verwey–Overbeek (DLVO) theory, which has already been employed to describe the self-assembly of charged gold NCs.^[11] On the other hand, the changes in the excitonic features of seemingly identical solvogels based on CdSe NCs with different inorganic capping ligands imply the presence of more complex interactions between the NCs, the capping ligands, and the linkers in the assembled structure. These interactions may not only be electrostatic in nature, as described by the DLVO theory, and thus can lead to completely new functionalities (Figure S2).

To prepare an aerogel from a CdSe NC wet gel, first, MFA was replaced with acetone followed by supercritical drying of the resulting solvogel according to a previously published procedure^[7b] to prevent the fine nanostructure from collapsing and to obtain the self-supporting aerogel monolith, whose scanning electron microscopy (SEM) image is displayed in Figure 3a. The absorption, steady-state, and time-resolved PL spectra of the CdSe NCs before and after surface modification with I[−], the CdSe(I[−])/Cd²⁺ solvogels in MFA, and the corresponding aerogels before and after activation in vacuum (at 120 °C for 24 h; this sample was further used for BET measurements) are shown in Figure 3b,c,f.

In all cases, the excitonic features were retained, aside from small shifts and broadening of the peaks, especially for the CdSe aerogel. The PL is first quenched upon ligand exchange with iodides and then partly restored in the

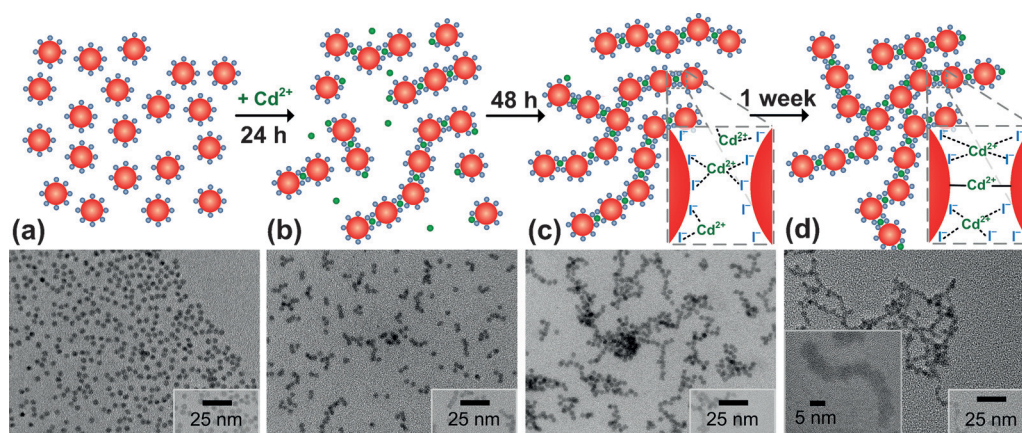


Figure 2. Schematic representation of the gelation process and TEM images showing the gelation of CdSe(I[−]) NCs (a) 24 h (b), 48 h (c), and 1 week (d) after the addition of Cd²⁺ linker.

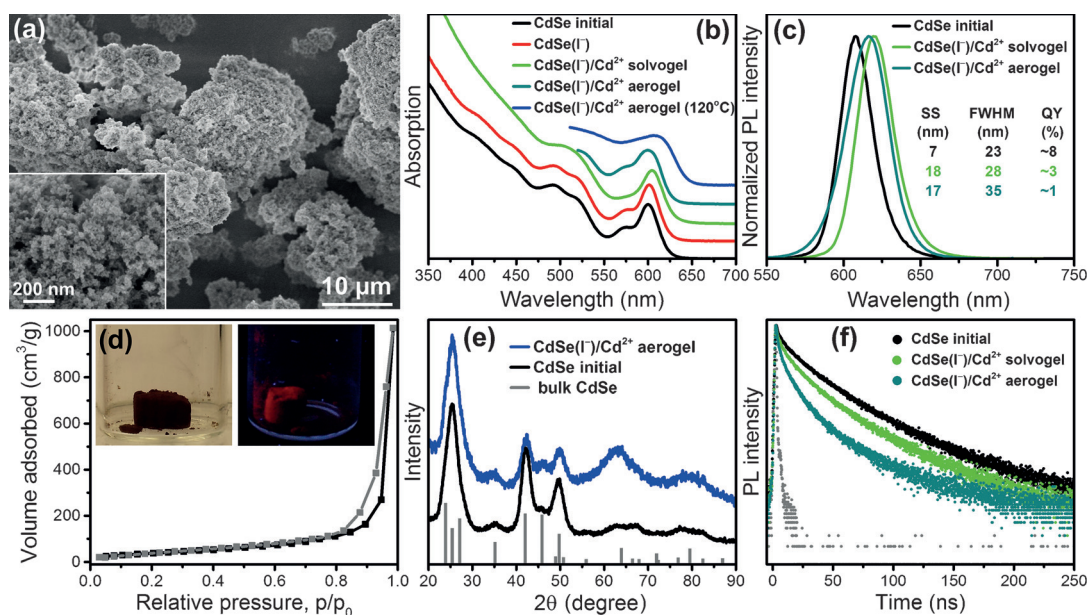


Figure 3. a) SEM image of an I^- -capped CdSe NC aerogel linked with Cd^{2+} ions. b) Absorption spectra of the CdSe NCs before and after the ligand exchange with I^- , their subsequent gelation with Cd^{2+} in MFA, and after drying and heat treatment of the resulting aerogel. The spectra were vertically shifted for clarity. c) PL spectra of the original CdSe NCs, the $\text{CdSe}(\text{I}^-)/\text{Cd}^{2+}$ wet gel, and the aerogel as well as their corresponding Stokes shifts, FWHM, and PLQY. d) The nitrogen physisorption isotherms of the $\text{CdSe}(\text{I}^-)/\text{Cd}^{2+}$ aerogel. The inset shows photographs of a CdSe aerogel monolith in daylight (left) and under UV light (right; PLQY $\approx 1\%$). e) XRD patterns of the original CdSe NCs and the all-inorganic CdSe NC aerogel. The experimental patterns are compared to the database powder diffractogram of wurtzite CdSe (CCD No. 9011664). f) Time-resolved PL spectra of the organic-capped CdSe NCs, the $\text{CdSe}(\text{I}^-)/\text{Cd}^{2+}$ wet gel, and the aerogel.

solvogel, implying that Cd^{2+} ions can act as both linkers and a passivating agents, suppressing non-radiative recombination processes induced by the anions (quantum yield (QY) ca. 3%). At the same time, the PL maximum shifted to longer wavelengths (by 8 nm), which is likely due to a favorable exciton energy transfer from smaller (donor) to larger (acceptor) NCs. A slight shift to higher energies and a peak broadening accompanied by a decrease in PL (QY ca. 1%) occurred after extensive washing, which is probably due to partial surface etching, ligand desorption, and larger size distributions. The changes in the QYs are in agreement with the time-resolved PL data. The decrease in the PL lifetime from the organic-capped CdSe NCs to the solvovogel and further to the aerogel was attributed to the formation of more channels for nonradiative deactivation through energy transfer and fast recombination on the non-passivated surface states. The latter is especially pronounced in the aerogel. Heat treatment of the aerogel results in complete PL quenching and broadening of the first excitonic peak. This can be explained by a strengthening of the electronic coupling between the NCs through their partial interfusion, and by the influence of dipole–dipole interactions and/or other factors related to the NC size distribution. Interestingly, the aerogels based on $\text{CdSe}(\text{I}^-)$ NCs linked with Zn^{2+} or Pb^{2+} ions showed optical properties that significantly differed from those linked with Cd^{2+} ions and much lower QYs (ca. 0.5% and < 0.1% vs. 3%, respectively), confirming the importance of the chemical similarity of the cations.

The increase in the cadmium content in the $\text{CdSe}(\text{I}^-)/\text{Cd}^{2+}$ aerogel compared to the initial $\text{CdSe}(\text{I}^-)$ NCs additionally

confirms the linking role of Cd^{2+} in the formation of the network (Table S3). Powder X-ray diffraction (XRD) analysis revealed no structural rearrangements in the gel formation process (Figure 3e). Thermogravimetric scans of the 4.5 nm $\text{CdSe}(\text{I}^-)$ NCs and the Cd^{2+} -linked aerogel showed total weight losses of 10% and 5%, respectively, which were significantly smaller than that of 24% for the organic-capped CdSe NCs (Figure S8).

The resulting $\text{CdSe}(\text{I}^-)/\text{Cd}^{2+}$ aerogel exhibited a remarkably large surface area of $146 \text{ m}^2 \text{ g}^{-1}$ (determined by nitrogen adsorption–desorption with BET analysis; Figure 3d). The isotherm resembles a type II curve with a sharp upturn at high relative pressures, which is characteristic for CdSe aerogels as reported by Brock and co-workers.^[3c] This sharp upturn (lack of saturation) is indicative of liquid condensation associated with the presence of macropores. A SEM image of the CdSe aerogel revealed the formation of a sponge-like 3D structure.

In conclusion, the approach developed to form all-inorganic 3D assemblies based on a variety of NCs represents a powerful method to tackle a crucial problem in technological applications of NCs, namely how to build well-interconnected all-inorganic 3D structures while retaining the characteristic properties of the individual NCs. The formation of a $\text{CdSe}(\text{I}^-)/\text{Cd}^{2+}$ aerogel was taken as an example. We showed that this highly porous solid of chemically interconnected NCs still exhibited well pronounced features of the individual quantum dots. We further demonstrated that the proposed versatile gelation approach is applicable to a wide range of semiconductor NCs with different morphologies, compositions, and sizes. This

method will undoubtedly enable the synthesis of materials for (opto)electronic applications, sensing, catalysis, and thermoelectrics.

Acknowledgements

This work was supported by the Deutsche Forschungsgemeinschaft (DFG) within the Cluster of Excellence “Center for Advancing Electronics Dresden” (cfAED) and by the European Research Council (ERC-2013-AdG project AEROCAT). We thank Nasser Mohamed-Noriega for help with the DLS measurements and Renate Schulze for the ICP-OES measurements.

Keywords: aerogels · gels · inorganic ligands · linked particles · semiconductor nanocrystals

How to cite: *Angew. Chem. Int. Ed.* **2016**, 55, 6334–6338
Angew. Chem. **2016**, 128, 6442–6446

-
- [1] a) C. B. Murray, C. R. Kagan, M. G. Bawendi, *Annu. Rev. Mater. Sci.* **2000**, 30, 545; b) M. V. Kovalenko, L. Manna, A. Cabot, Z. Hens, D. V. Talapin, C. R. Kagan, V. I. Klimov, A. L. Rogach, P. Reiss, D. J. Milliron, P. Guyot-Sionnest, G. Konstantatos, W. J. Parak, T. Hyeon, B. A. Korgel, C. B. Murray, W. Heiss, *ACS Nano* **2015**, 9, 1012; c) D. V. Talapin, J.-S. Lee, M. V. Kovalenko, E. V. Shevchenko, *Chem. Rev.* **2010**, 110, 389.
- [2] J. J. Urban, D. V. Talapin, E. V. Shevchenko, C. R. Kagan, C. B. Murray, *Nat. Mater.* **2007**, 6, 115.
- [3] a) N. Gaponik, A.-K. Herrmann, A. Eychmüller, *J. Phys. Chem. Lett.* **2012**, 3, 8; b) J. L. Mohanan, I. U. Arachchige, S. L. Brock, *Science* **2005**, 307, 397; c) I. U. Arachchige, S. L. Brock, *Acc. Chem. Res.* **2007**, 40, 801; d) W. Liu, A.-K. Herrmann, N. C. Bigall, P. Rodriguez, D. Wen, M. Oezaslan, T. J. Schmidt, N. Gaponik, A. Eychmüller, *Acc. Chem. Res.* **2015**, 48, 154; e) C. Zhu, D. Du, A. Eychmüller, Y. Lin, *Chem. Rev.* **2015**, 115, 8896; f) S. Sánchez-Paradinas, D. Dorfs, S. Friebe, A. Freytag, A. Wolf, N. C. Bigall, *Adv. Mater.* **2015**, 27, 6152; g) A. Freytag, S. Sánchez-Paradinas, S. Naskar, N. Wendt, M. Colombo, G. Pugliese, J. Poppe, C. Demirci, I. Kretschmer, D. W. Bahnemann, P. Behrens, N. C. Bigall, *Angew. Chem. Int. Ed.* **2016**, 55, 1200; *Angew. Chem.* **2016**, 128, 1217.
- [4] a) M. V. Kovalenko, M. Scheele, D. V. Talapin, *Science* **2009**, 324, 1417; b) A. Nag, M. V. Kovalenko, J.-S. Lee, W. Liu, B. Spokoyny, D. V. Talapin, *J. Am. Chem. Soc.* **2011**, 133, 10612; c) V. Sayevich, N. Gaponik, M. Plötner, M. Kruszynska, T. Gemming, V. M. Dzhagan, S. Akhavan, D. R. T. Zahn, H. V. Demir, A. Eychmüller, *Chem. Mater.* **2015**, 27, 4328; d) A. T. Fafarman, W.-k. Koh, B. T. Diroll, D. K. Kim, D.-K. Ko, S. J. Oh, X. Ye, V. Doan-Nguyen, M. R. Crump, D. C. Reifsnyder, C. B. Murray, C. R. Kagan, *J. Am. Chem. Soc.* **2011**, 133, 15753; e) S. J. Oh, N. E. Berry, J.-H. Choi, E. A. Gauding, H. Lin, T. Paik, B. T. Diroll, S. Muramoto, C. B. Murray, C. R. Kagan, *Nano Lett.* **2014**, 14, 1559.
- [5] A. Nag, D. S. Chung, D. S. Dolzhnikov, N. M. Dimitrijevic, S. Chattopadhyay, T. Shibata, D. V. Talapin, *J. Am. Chem. Soc.* **2012**, 134, 13604.
- [6] a) D. S. Dolzhnikov, H. Zhang, J. Jang, J. S. Son, M. G. Panthani, T. Shibata, S. Chattopadhyay, D. V. Talapin, *Science* **2015**, 347, 425; b) J.-H. Choi, A. T. Fafarman, S. J. Oh, D.-K. Ko, D. K. Kim, B. T. Diroll, S. Muramoto, J. G. Gillen, C. B. Murray, C. R. Kagan, *Nano Lett.* **2012**, 12, 2631.
- [7] a) T. Hendel, V. Lesnyak, L. Kühn, A.-K. Herrmann, N. C. Bigall, L. Borchardt, S. Kaskel, N. Gaponik, A. Eychmüller, *Adv. Funct. Mater.* **2013**, 23, 1903; b) N. Gaponik, A. Wolf, R. Marx, V. Lesnyak, K. Schilling, A. Eychmüller, *Adv. Mater.* **2008**, 20, 4257.
- [8] a) V. Lesnyak, S. V. Voitekhovich, P. N. Gaponik, N. Gaponik, A. Eychmüller, *ACS Nano* **2010**, 4, 4090; b) V. Lesnyak, A. Wolf, A. Dubavik, L. Borchardt, S. V. Voitekhovich, N. Gaponik, S. Kaskel, A. Eychmüller, *J. Am. Chem. Soc.* **2011**, 133, 13413; c) A. Wolf, V. Lesnyak, N. Gaponik, A. Eychmüller, *J. Phys. Chem. Lett.* **2012**, 3, 2188; d) S. V. Voitekhovich, V. Lesnyak, N. Gaponik, A. Eychmüller, *Small* **2015**, 11, 5728.
- [9] A. Singh, B. A. Lindquist, G. K. Ong, R. B. Jadrich, A. Singh, H. Ha, C. J. Ellison, T. M. Truskett, D. J. Milliron, *Angew. Chem. Int. Ed.* **2015**, 54, 14840; *Angew. Chem.* **2015**, 127, 15053.
- [10] V. Sayevich, C. Guhrenz, M. Sin, V. M. Dzhagan, A. Weiz, D. Kasemann, E. Brunner, M. Ruck, D. R. T. Zahn, K. Leo, N. Gaponik, A. Eychmüller, *Adv. Funct. Mater.* **2016**, 26, 2163.
- [11] H. Zhang, D. Wang, *Angew. Chem. Int. Ed.* **2008**, 47, 3984; *Angew. Chem.* **2008**, 120, 4048.

Received: January 5, 2016

Published online: April 21, 2016